Optimal Maneuvers Using a Three Dimensional Gravity Assist

G. Felipe and A.F.B.A. Prado

Instituto Nacional de Pesquisas Espaciais,
São José dos Campos, 12227-010, Brazil

Abstract: In the present paper the swing-by maneuvers are studied and classified under the model given by the three-dimensional restricted three-body problem. The modification in the orbit of the spacecraft due to the close approach is shown in plots that specify from which type of orbits the spacecraft is coming and to which type it is going. The results generated here are used to solve optimal problems, such as finding trajectories that satisfy some given constraints (such as achieving an escape or a capture) with some parameters being extremized (position, velocity, etc...).

Keywords: *Astrodynamics; swing-by; orbital maneuvers; gravity-assist; restricted problem.*

Mathematics Subject Classification (2000): 70M20, 70Q05.

1 Introduction

Applications of the swing-by technique can be found in several publications in the literature $[1-9]$. In the present paper the swing-by maneuvers are studied and classified under the model given by the three-dimensional circular restricted three-body problem. The goal is to simulate a large variety of initial conditions for those orbits and classify them according to the effects caused by the close approach in the orbit of the spacecraft. This swing-by is assumed to be performed around the secondary body of the system. For a large number of values of these three variables, the equations of motion are integrated numerically forward and backward in time, until the spacecraft is at a distance that can be considered far enough from M_2. It is necessary to integrate in both directions of time because the set of initial conditions used gives information about the spacecraft exactly at the moment of the closest approach. At these two points, the effect of M_2 can be neglected and the system formed by M_1 and the spacecraft can be considered a two-body system. At these two points, two-body celestial mechanics formulas are valid

to compute the energy and the angular momentum before and after the close approach. With those results, the orbits are classified in four categories: elliptic direct (negative energy and positive angular momentum), elliptic retrograde (negative energy and angular momentum), hyperbolic direct (positive energy and angular momentum) and hyperbolic retrograde (positive energy and negative angular momentum). Then, the problem is to identify the category of the orbit of the spacecraft before and after the close encounter with M_2. After that, those results are used to identify up to sixteen classes of transfers, accordingly to the changes in the category of the orbit caused by the close encounter. They are named with the first sixteen letters of the alphabet. After that, several optimal problems involving this maneuver can be formulated and solved with the help of the plots shown. Some examples include finding specific types of orbits (escape, capture, etc.) that have maximum or minimum velocity at periapsis (or any other parameters, such as the distance of the periapsis or the angle of approach).

2 The Swing-By in Three Dimensions

This maneuver can be identified by four independent parameters: i) V_p, the magnitude of the velocity of the spacecraft at periapsis. For the most general case, it would be necessary to give an information about the direction of the velocity. In this paper, only velocities parallel to the x–y plane are considered. This constraint is assumed, because it is the most usual situation in interplanetary research, since the planets have orbits that are almost coplanar. Under this approximation, and taking into account that the velocity at periapse is perpendicular to the periapsis vector, the information about the magnitude of the velocity is enough to completely specify the velocity vector; ii) R_p, the distance between the spacecraft and the celestial body during the closest approach; iii) α, the angle between the projection of the periapsis line in the x–y plane and the line that connects the two primaries; iv) β, the angle between the periapsis line and the x–y plane.
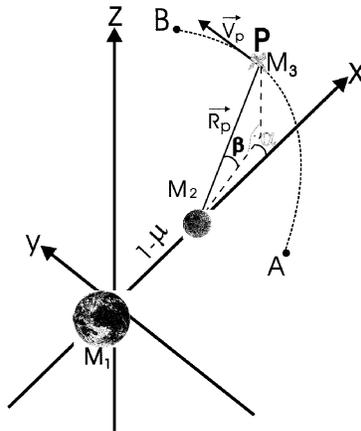

Figure 2.1.   The swing-by in the three-dimensional space.

Figure 2.1 shows the sequence for this maneuver and some of those and other important variables. It is assumed that the system has three bodies: a primary (M_1) and a secondary (M_2) body with finite masses that are in circular orbits around their common center of mass and a third body with negligible mass (the spacecraft) that has its motion governed by the two other bodies. The spacecraft leaves the point A, passes by the point P (the periapsis of the trajectory of the spacecraft in its orbit around M_2) and goes to the point B. The points A and B are chosen in a such way that the influence of M_2 at those two points can be neglected and, consequently, the energy can be assumed to remain constant after B and before A (the system follows the two-body celestial mechanics). The initial conditions are clearly identified in the Figure 2.1: the periapsis distance R_p (distance measured between the point P and the center of M_2), the angles α and β and the velocity V_p. The distance R_p is not to scale, to make the figure easier to understand. The result of this maneuver is a change in velocity, energy and angular momentum in the keplerian orbit of the spacecraft around the central body.

3 The Three-Dimensional Circular Restricted Problem

For the research performed in this paper, the equations of motion for the spacecraft are assumed to be the ones valid for the well-known three-dimensional restricted circular three-body problem. The standard dimensionless canonical system of units is used, which implies that: the unit of distance is the distance between M_1 and M_2; the mean angular velocity (ω) of the motion of M_1 and M_2 is assumed to be one; the mass of the smaller primary (M_2) is given by $\mu = \frac{m_2}{m_1+m_2}$ (where m_1 and m_2 are the real masses of M_1 and M_2, respectively) and the mass of M_2 is $(1-\mu)$; the unit of time is defined such that the period of the motion of the two primaries is 2π and the gravitational constant is one. There are several systems of reference that can be used to describe the three-dimensional restricted three-body problem [10; Chapter 10]. In this paper the rotating system is used. In this system of reference, the origin is the center of mass of the two massive primaries. The horizontal axis (x) is the line that connects the two primaries at any time. It rotates with a variable angular velocity in a such way that the two massive primaries are always on this axis. The vertical axis (y) is perpendicular to the (x) axis. In this system, the positions of the primaries are: $x_1 = -\mu$, $x_2 = 1 - \mu$, $y_1 = y_2 = 0$. In this system, the equations of motion for the massless particle are [10; Chapter 10]:

$$\ddot{x} - 2\dot{y} = x - (1-\mu)\frac{x+\mu}{r_1^3} - \mu\frac{x-1+\mu}{r_2^3}, \tag{1}$$

$$\ddot{y} + 2\dot{x} = y - (1-\mu)\frac{y}{r_1^3} - \mu\frac{y}{r_2^3}, \tag{2}$$

$$\ddot{z} = -(1-\mu)\frac{z}{r_1^3} - \mu\frac{z}{r_2^3}, \tag{3}$$

where r_1 and r_2 are the distances from M_1 and M_2.

4 Algorithm to Solve the Problem

A numerical algorithm to solve the problem has the following steps: 1. Arbitrary values for the three parameters R_p, V_p, α and β are given; 2. With these values the initial

conditions in the rotating system are computed. The initial position is the point (X_i, Y_i, Z_i) and the initial velocity is (V_{Xi}, V_{Yi}, V_{Zi}), where:

$$X_i = 1 - \mu + R_p \cos(\beta) \cos(\alpha), \tag{4}$$

$$Y_i = R_p \cos(\beta) \sin(\alpha), \tag{5}$$

$$Z_i = R_p \sin(\beta), \tag{6}$$

$$V_{Xi} = -V_p \sin(\alpha) + R_p \cos(\beta) \sin(\alpha), \tag{7}$$

$$V_{Yi} = V_p \cos(\alpha) - R_p \cos(\beta) \cos(\alpha), \tag{8}$$

$$V_{Zi} = 0, \tag{9}$$

where the last equation comes from the decision of studying the maneuvers with V_p parallel to the orbital plane of the primaries; 3. With these initial conditions, the equations of motion are integrated forward in time until the distance between M_2 and the spacecraft is larger than a specified limit d. At this point the numerical integration is stopped and the energy (E_+) and the angular momentum (C_+) after the encounter are calculated; 4. Then, the particle goes back to its initial conditions at the point P, and the equations of motion are integrated backward in time, until the distance d is reached again. Then the energy (E_-) and the angular momentum (C_-) before the encounter are calculated.

For all the simulations shown, a Runge–Kutta of 8th order was used for numerical integration. The criteria to stop numerical integration is the distance between the spacecraft and M_2. When this distance reaches the value $d = 0.5$ (half of the semimajor axis of the two primaries) the numerical integration is stopped. The value 0.5 is larger than the sphere of influence of M_2, which avoids any important effects of M_2 at these points. Simulations using larger values for this distance were performed, and it increased the integration time, but did not significantly change the results. To study the effects of numerical accuracy, several cases were simulated using different integration methods and/or different values for the accuracy required with no effects in the results.

With this algorithm available, the given initial conditions (values of R_p, V_p, α, β) are varied in any desired range and the effects of the close approach in the orbit of the spacecraft are studied.

5 Classification of the Orbits

The main results consist of plots that show the change of the orbit of the spacecraft, due to the close encounter with M_2. The Earth–Moon, Sun–Uranus and the Sun–Saturn systems of primaries are used. Any mission using a swing-by with one of those system can use those results. First of all, it is necessary to classify all the close encounters between M_2 and the spacecraft, according to the change obtained in the orbit of the spacecraft. The letters A–P are used for this classification. They are assigned to the orbits according to the rules showed in Table 5.1.

With those rules defined, the results consist of assigning one of those letters to a position in a two-dimensional diagram that has the angle α (in degrees) in the vertical axis and the angle β (in degrees) in the horizontal axis. One plot is made for every value of R_p and V_p. This type of diagram is called here a "letter-plot" and it was used before in [2].

Table 5.1. Rules to assign letters to orbits.

After Before	Direct Ellipse	Retrograde Ellipse	Direct Hyperbola	Retrograde Hyperbola
Direct Ellipse	A	E	I	M
Retrograde Ellipse	B	F	J	N
Direct Hyperbola	C	G	K	O
Retrograde Hyperbola	D	H	L	P

In the present paper several simulations were made and they are shown in Figures 5.1–5.3. For each plot a total of 961 trajectories were generated, dividing each axis in 31 segments. The interval plotted for α is $180 \leq \alpha \leq 360 \, deg$ because there is a symmetry with respect to the vertical line $\alpha = 180 \, deg$. The plot for the interval $0 \leq \alpha \leq 180 \, deg$ is a mirror image of the region $180 \leq \alpha \leq 360 \, deg$ with the following letter substitutions: L becomes O, N becomes H, I becomes C, B becomes E, M becomes D and J becomes G. The letters K, P, F and A remain unchanged.
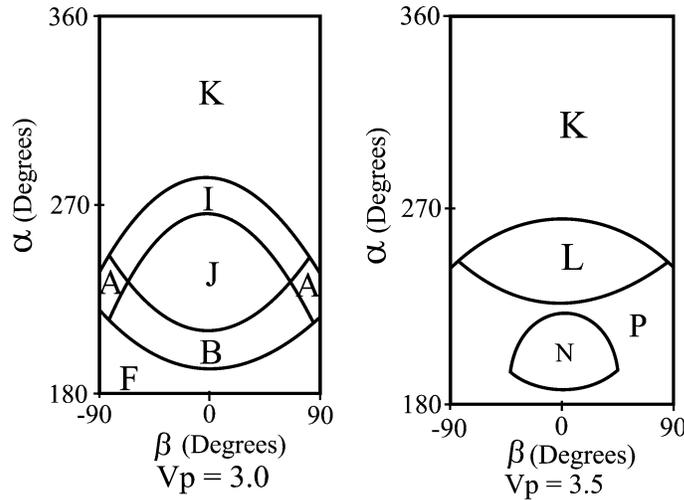

Figure 5.1.   Simulations for $R_p = 0.00008464$ in the Sun–Saturn system.

By examining Figures 5.1–5.3 it is possible to identify the following families of orbits: a) Orbits that result in an escape (transfer from elliptic to hyperbolic), that are represented by the letters I, J, M, N and that appear between the center ($\alpha = 270°$) and the bottom part of some of the plots (the ones for lower velocities); b) Orbits that result in a capture (transfer from hyperbolic to elliptic), that are represented by the letters C, D, G, H that do not appear in the plots shown in this paper (but exist in the symmetric part not shown here); c) Elliptic orbits (transfer from elliptic to elliptic), that are represented by the letters A, B, E, F and that appear at the bottom of some of the plots (the ones for lower velocities); d) Hyperbolic orbits (transfer from hyperbolic to hyperbolic), that
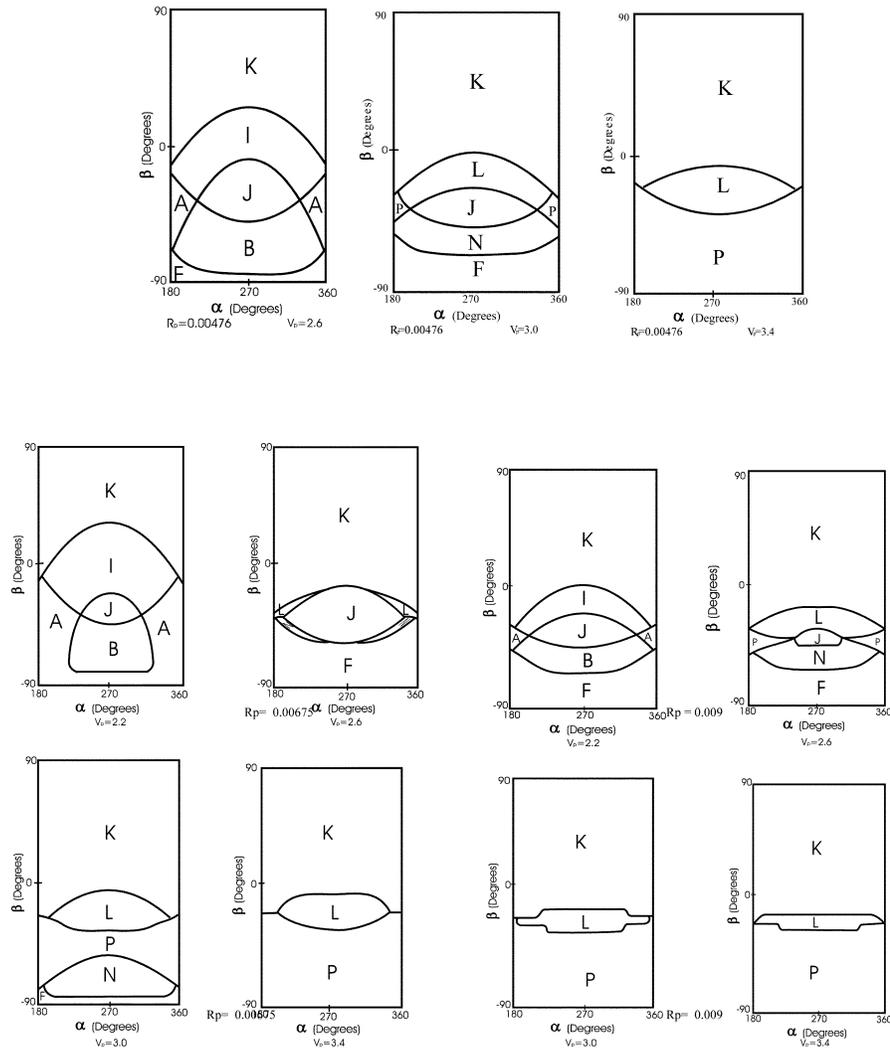
Figure 5.2. Simulations in the Earth–Moon system.

are represented by the letters K, L, O, P and that appears at the upper part of the plots and that are the only families available for higher velocities; e) Orbits that change the direction of motion from direct to retrograde that are represented by the letters E, M, G, O and that do not appear in the plots shown in this paper (but exist in the symmetric part not shown here); f) Orbits that change the direction of motion from retrograde to direct, that are represented by the letters B, D, J, L, that appear in the lower-center of the plot; g) Retrograde orbits that are represented by the letters F, H, N, P that appear in the majority of the bottom part of the plots; h) Direct orbits that are represented by the letters A, C, I, K that appear in the top of the plots.
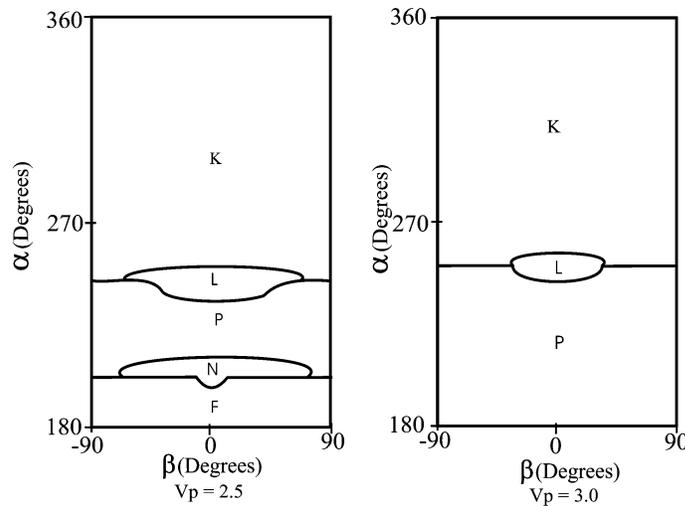
Figure 5.3.   Simulations for $R_p = 0.000082$ in the Sun–Uranus system.

6 Optimal Problems

The results generated in this research can be used to help mission designers to plan missions that involve optimization of parameters. It is possible to use the plots made here to find situations where a specific case (represented by the letters A–P) can be obtained with one or more variables (like V_p or R_p) extremized. The parameters V_p and R_p are important parameters to be extremized. If the goal of the mission is to collect data from M_2, it is interesting to minimize R_p (to get closer to M_2) and V_p (to stay more time close to M_2). In the opposite, if M_2 is necessary to be used to change the trajectory of the spacecraft, but it represents a risk to the vehicle due to the presence of an atmosphere and/or radiation, etc., it is necessary to maximize R_p and/or V_p, subject to the restriction of obtaining the desired change in the trajectory. To use a real case as an example, the Earth–Moon, Sun–Saturn and the Sun–Uranus systems are used to solve the problems described below.

Problem 1: It is desired to find a trajectory of type N (a retrograde escape) in the Earth–Moon system, subject to the constraints $V_p = 3.0$ and requiring that R_p is maximized. Figure 5.2 shows that the trajectory type N, in the case $V_p = 3.0$, appear for $R_p = 0.00476$ and $R_p = 0.00675$, but do not appear for $R_p = 0.009$. Figure 6.1 shows plots of the sequence made to find the solution. The solution to this problem is $R_p = 0.0075234375$. The complete values for the set of variables are: $\alpha = 192°$; $\beta = 0°$.

Problem 2: It is desired to find a trajectory of type B (an ellipse that changes the motion from retrograde to direct) in the Sun–Saturn system, subject to the constraints $R_p = 0.00008464$ (2.0 radius of Saturn) and requiring that the velocity at periapsis be a maximum. Figure 5.1 shows that the trajectory type B appears for $V_p = 3.0$, but do not appear for $V_p = 3.5$. To find the solution, plots were made for several values of V_p in this interval. Figure 6.2 shows two plots of this sequence. The solution to this problem is $V_p = 3.12$, since for $V_p = 3.13$, B does not occur anymore. It is also possible to see that this problem has four solutions: $\alpha = 216°$, $\beta = -54°$; $\alpha = 210°$, $\beta = -24°$; $\alpha = 210°$, $\beta = 24°$; $\alpha = 216°$, $\beta = 54°$.
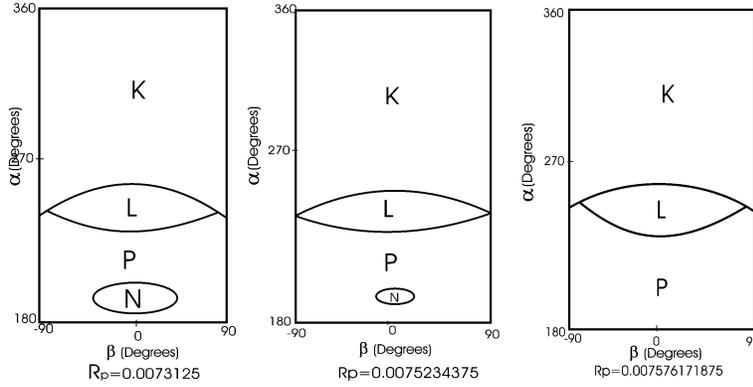
Figure 6.1.   Solution for the Problem 1 in the Earth–Moon system.
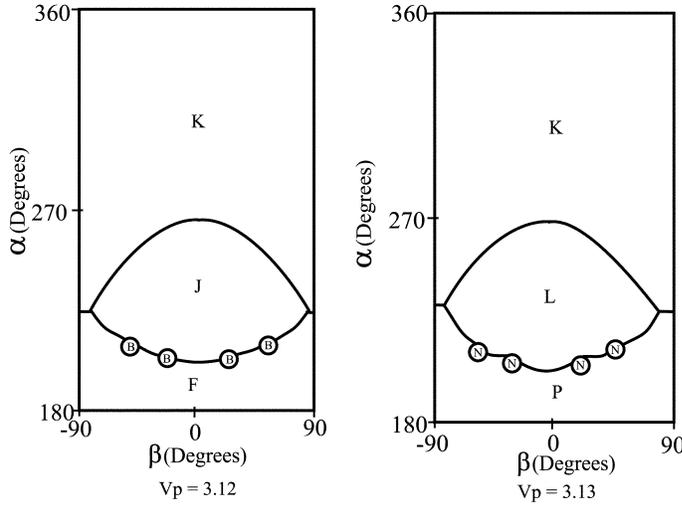

Figure 6.2.   Solution for the Problem 2 for $R_p = 0.00008464$ in the Sun–Saturn system.

Problem 3: It is desired to obtain a trajectory of type N (a retrograde ellipse before the swing-by and a retrograde hyperbola after) in the Sun–Uranus system, subject to the constraints $R_p = 0.000082$ (10.0 radius of Uranus) and requiring that the velocity at periapsis be a maximum. Figure 5.3 shows that the trajectory type N appears for $V_p = 2.5$, but do not appear for $V_p = 3.0$. To find the solution, plots were made for several values of V_p in this interval. Figure 6.3 shows two plots of this sequence. The solution to this problem is $V_p = 2.62$, since for $V_p = 2.63$, N does not occur anymore. In this example, it is possible to see that there is a range of values of β that allows solutions. So, the complete values for the set of variables are: $-48° \leq \beta \leq 48°$; $\alpha = +186°$.

   This information constitutes a set of initial conditions to design the trajectory. Several improvements can be made: 1) more plots can be generated to get more accuracy for the data, in particular in the solutions of the optimal problems; 2) many other types of
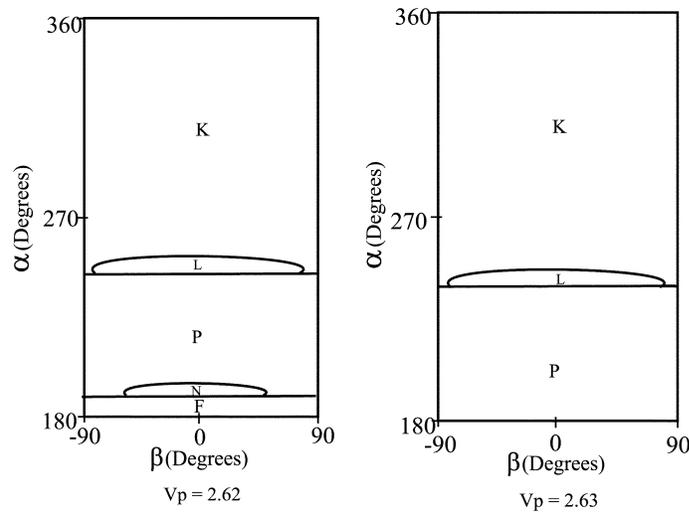
Figure 6.3.   Solution for the Problem 3 for $R_p = 0.000082$ in the Sun–Uranus system.

optimization problems can be solved, combining different constraints and/or variables to be extremized; 3) others systems can be used; etc.

7 Conclusions

In this paper the three-dimensional restricted three-body problem is described and used to study the swing-by maneuver. Several letter-plot type of graphics are made to represent the effect of a close approach in the orbit of a spacecraft. In particular, the effects of the third dimension in this maneuver are studied. It is shown that the hyperbolic orbits (family K) dominate the region where α is larger than 270° and that when the velocity increases, the families K, L and P dominate the plots. Families with particularities, like parabolic or zero angular momentum orbits, are shown to exist in the borders between the main families. After that, the results available here were used in the solution of optimal problems. In this type of problem, it is necessary to find the initial conditions that generates a given orbit change, subject to the extremization of some parameters like V_p or R_p.

References

[1] Broucke, R.A. and Prado, A.F.B.A. Jupiter swing-by trajectories passing near the Earth. *Advances in the Astronautical Sciences* **82**(2) (1993) 1159–1176.
[2] Broucke, R.A. The celestial mechanics of gravity assist. In: *AIAA/AAS Astrodynamics Conference, Minneapolis, MN, 15–17 August*, Paper 88-4220, 1988.
[3] D'Amario, L.A., Byrnes, D.V. and Stanford, R.H. A new method for optimizing multiple-flyby trajectories. *Journal of Guidance, Control, and Dynamics* **4**(6) (1981) 591–596.
[4] D'Amario, L.A., Byrnes, D.V. and Stanford, R.H. Interplanetary trajectory optimization with application to galileo. *Journal of Guidance, Control, and Dynamics* **5**(5) (1982) 465–471.

[5] Farquhar, R.W. and Dunham, D.W. A new trajectory concept for exploring the Earth's geomagnetic tail. *Journal of Guidance, Control and Dynamics* **4**(2) (1981) 192–196.

[6] Felipe, G. and Prado, A.F.B.A. Classification of out of plane swing-by trajectories. *Journal of Guidance, Control and Dynamics* **22**(5) (1999) 643–649.

[7] Flandro, G. Fast reconnaissance missions to the outer solar system utilizing energy derived from the gravitational field of Jupiter. *Astronautical Acta* **12**(4) (1966) 329–337.

[8] Muhonen, D., Davis, S. and Dunham, D. Alternative gravity-assist sequences for the ISEE-3 escape trajectory. *Journal of Astronautical Sciences* **33**(3) (1985) 255–273.

[9] Prado, A.F.B.A. Close-approach trajectories in the elliptic restricted problem. *Journal of Guidance, Control, and Dynamics* **20**(4) (1997) 797–802.

[10] Szebehely, V. *Theory of Orbits.* Academic Press, New York, 1967.